Extended spin–boson model for nonadiabatic hydrogen tunneling in the condensed phase

ARTICLE *in* THE JOURNAL OF CHEMICAL PHYSICS · NOVEMBER 2006

Impact Factor: 2.95 · DOI: 10.1063/1.2354500 · Source: PubMed

3 AUTHORS, INCLUDING:

Alexander V. Soudackov
University of Illinois, Urbana-Champaign
54 PUBLICATIONS **1,753** CITATIONS

Extended spin-boson model for nonadiabatic hydrogen tunneling in the condensed phase

Yasuhito Ohta, Alexander V. Soudackov, and Sharon Hammes-Schiffer[a)]
Department of Chemistry, Pennsylvania State University, University Park, Pennsylvania 16802

(Received 2 June 2006; accepted 21 August 2006; published online 13 October 2006)

A nonadiabatic rate expression for hydrogen tunneling reactions in the condensed phase is derived for a model system described by a modified spin-boson Hamiltonian with a tunneling matrix element exponentially dependent on the hydrogen donor-acceptor distance. In this model, the two-level system representing the localized hydrogen vibrational states is linearly coupled to the donor-acceptor vibrational mode and the harmonic bath. The Hamiltonian also includes bilinear coupling between the donor-acceptor mode and the bath oscillators. This coupling provides a mechanism for energy exchange between the two-level system and the bath through the donor-acceptor mode, thereby facilitating convergence of the time integral of the probability flux correlation function for the case of weak coupling between the two-level system and the bath. The dependence of the rate constant on the model parameters and the temperature is analyzed in various regimes. Anomalous behavior of the rate constant is observed in the weak solvation regime for model systems that lack an effective mechanism for energy exchange between the two-level system and the bath. This theoretical formulation is applicable to a wide range of chemical and biological processes, including neutral hydrogen transfer reactions with small solvent reorganization energies. © *2006 American Institute of Physics*. [DOI: 10.1063/1.2354500]

I. INTRODUCTION

Hydrogen transfer reactions are ubiquitous throughout chemistry and biology. Due to the relatively small mass of the hydrogen atom, quantum mechanical phenomena such as zero point energy and hydrogen tunneling effects are often important even at relatively high temperatures. For example, deuterium kinetic isotope effects as large as ~100 have been observed at room temperature for hydrogen abstraction reactions catalyzed by enzymes.[1–7] Such large kinetic isotope effects imply that the hydrogen transfer reaction proceeds by a nonadiabatic tunneling process.[8] The temperature dependences of the rate constants and kinetic isotope effects for these types of reactions exhibit a broad range of behavior.

A variety of theoretical descriptions of tunneling processes in condensed phases has been presented throughout the literature.[9,10] The early models for nonadiabatic hydrogen transfer reactions stemmed from the theory of nonradiative transitions in molecular crystals[11,12] and nonadiabatic electron transfer.[13–16] Many of the theoretical models for hydrogen tunneling emphasize the key role of the reorganization of the environment and the fluctuations of the donor-acceptor distance.[17–22] The interplay of different mechanisms for energy exchange between the tunneling system and the environment has also been explored.[23] The temperature dependence of the rate constant for the various models spans the range from the weak dependence characteristic of quantum processes at low temperatures to the exponential dependence characteristic of thermally activated processes.

The present work is related to the theories of hydrogen tunneling[19,24–28] based on the perturbation treatment of the spin-boson model widely used to study quantum processes in dissipative environments.[10] In this model, the hydrogen transfer system is composed of three subsystems: the two-level system (TLS) describing the two lowest localized quantum vibrational states of the hydrogen, the hydrogen donor-acceptor vibrational mode modulating the tunneling matrix element, and the bath (solvent or protein) environment represented as a collection of harmonic oscillators. The TLS is coupled to both the hydrogen donor-acceptor mode and the harmonic bath. The explicit coupling of the hydrogen donor-acceptor vibration to the hydrogen tunneling motion distinguishes hydrogen transfer reactions from the closely related electron transfer reactions and is responsible for many interesting phenomena, including non-Arrhenius temperature dependence of the rates at high temperatures,[26,27] activationless behavior at low temperatures with enhanced rates,[29] and temperature dependent isotope effects.[5,30–32]

The most complete analytical treatment of the spin-boson model for hydrogen transfer reactions was presented by Suarez and Silbey.[28] Using the golden rule formulation, they derived analytical expressions for the rate constant in various regimes and analyzed the rate and its temperature dependence in these regimes. Their treatment did not include explicit coupling between the hydrogen donor-acceptor vibrational motion and the bath oscillators, and the donor-acceptor vibrational mode was represented as an undamped harmonic oscillator. In the strong solvation regime, where the coupling between the TLS and the bath is large, this assumption does not lead to any complications.[19,33,34] In the case of extremely weak coupling between the TLS and the bath, however, this assumption could lead to poor conver-

[a)]Author to whom correspondence should be addressed. Electronic mail: shs@chem.psu.edu

gence of the time integral of the probability flux correlation function. If no energy dissipation mechanism is available for the tunneling system, the nonadiabatic transitions are purely coherent, and the rate is not well defined. The coupling between the TLS and the bath is expected to be weak for neutral hydrogen transfer reactions characterized by very small solvent reorganization energies.

In the present paper, we address this issue by including explicit bilinear coupling of the donor-acceptor mode to the bath modes in the spin-boson Hamiltonian. The coupling between the donor-acceptor mode and the bath provides an additional channel for energy exchange between the TLS and the bath through the donor-acceptor mode. As a result, the convergence of the time integral of the probability flux correlation function is facilitated, particularly in the case of very weak coupling between the TLS and the bath. Furthermore, this Hamiltonian provides a more realistic description of hydrogen tunneling in chemical and biological systems, where the donor-acceptor mode is typically coupled to the solvent or protein environment. The importance of such coupling in biological hydrogen transfer systems has been pointed out previously.[35] Here we derive a nonadiabatic rate expression for this spin-boson Hamiltonian and apply it to a series of model systems. Our analyses of the various terms in the nonadiabatic rate expression and the results for model systems provide insights into the fundamental physical principles underlying these types of processes.

This paper is organized as follows. Section II presents the theoretical formulation. In the initial part of this section, the general model for hydrogen tunneling in a dissipative environment is discussed, and the spin-boson Hamiltonian is defined. The main part of this section presents the derivation of the nonadiabatic rate expression. Section III describes the application of this theoretical formulation to a series of model systems. The dependence of the rate constant on the donor-acceptor mode frequency, the coupling between the donor-acceptor mode and the bath, and the temperature is analyzed for both the strong and weak solvation regimes. The summary and conclusions are provided in Sec. IV.

II. THEORETICAL FORMULATION

A. General model system

The model used in this paper consists of a reactive donor-hydrogen-acceptor subsystem immersed in a thermal bath representing a solvent or protein environment. The relevant nuclear degrees of freedom in the system are the coordinate of the transferring hydrogen atom, the distance between the hydrogen donor and acceptor atoms, and the coordinates of the bath. In the Born-Oppenheimer approximation, the motion of the hydrogen occurs on the electronic ground state adiabatic potential energy surface $V_{\mathrm{H}}(q_{\mathrm{H}};Q,\{q_j\})$, where q_{H} is the hydrogen coordinate, Q is the distance between the hydrogen donor and acceptor, and $\{q_j\}=q_1,q_2,\ldots,q_N$ represent N degrees of freedom of the bath. The hydrogen potential $V_{\mathrm{H}}(q_{\mathrm{H}};Q,\{q_j\})$ depends parametrically on the coordinates Q and $\{q_j\}$, as illustrated in Fig. 1. The bath coordinates $\{q_j\}$ mainly impact the relative energies of the donor and acceptor wells of the double well potential. Thermal fluctuations of the bath coordinates lead to a symmetric double well potential that enables hydrogen tunneling. The donor-acceptor coordinate Q mainly impacts the barrier height and width of the double well potential. As Q becomes larger, the barrier height and width increase, and the hydrogen tunneling splitting decreases.

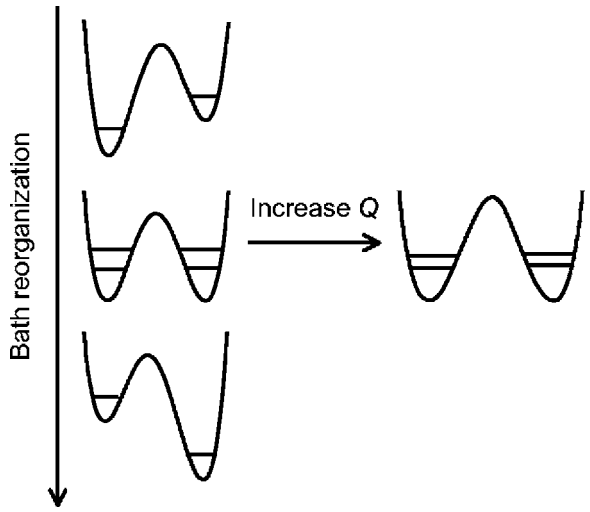

FIG. 1. Schematic picture of a general hydrogen tunneling system. The double well potential energy curves are functions of the hydrogen coordinate q_{H}, and the lowest two adiabatic hydrogen vibrational states are depicted for each hydrogen potential energy curve. Reorganization of the bath environment alters the relative energies of the wells of the hydrogen potential energy curves. Hydrogen tunneling is allowed for the symmetric double well potential. Increasing the donor-acceptor distance Q increases the barrier height and width, thereby decreasing the tunneling splitting between the adiabatic hydrogen vibrational states. In the diabatic representation, the bath reorganization leads to degeneracy of the reactant and product diabatic states, and the nonadiabatic coupling between these states decreases as the donor-acceptor distance Q increases.

For the relatively high potential barrier case, we can define the sets of reactant and product vibrational states $\{|R_n\rangle,|P_n\rangle\}$ localized in the left and right wells, respectively. For typical hydrogen vibrational frequencies of $\sim$3000 cm^{-1}, the energy splittings within each well are substantially larger than the thermal energy $k_{\mathrm{B}}T$ at ambient temperatures, and we can ignore transitions between the states within the reactant and product sets. Thus, only the two ground states $|R\rangle \equiv |R_0\rangle$ and $|P\rangle \equiv |P_0\rangle$ are considered, and the multilevel system is reduced to a TLS.[36] The eigenenergies associated with the two ground states are denoted $E_R(Q,\{q_j\})$ and $E_P(Q,\{q_j\})$. In this reduced system, hydrogen tunneling is described by quantum transitions from state $|R\rangle$ to state $|P\rangle$ induced by the tunneling matrix element (nonadiabatic coupling) V. Thermal fluctuations in the bath coordinates lead to the degeneracy of the two diabatic states $|R\rangle$ and $|P\rangle$, and the nonadiabatic coupling V determines the tunneling splitting between the adiabatic states depicted in Fig. 1. The nonadiabatic coupling V depends strongly on the donor-acceptor coordinate Q.

The eigenenergies $E_R(Q,\{q_j\})$ and $E_P(Q,\{q_j\})$ can be regarded as diabatic potential energy surfaces for the vibrationally nonadiabatic hydrogen transfer reaction occurring on the electronically adiabatic ground state. Expanding these surfaces in a Taylor series in terms of Q and $\{q_j\}$ around the

reactant and product equilibrium configurations $(\bar{Q}_\sigma, \{\bar{q}_\sigma^{(j)}\})$ $(\sigma = R, P)$ and retaining the terms up to second order we obtain the following harmonic approximation:

$$
\begin{aligned}
&E_\sigma(Q,\{q_j\}) \\
&\quad = E_\sigma(\bar{Q}_\sigma,\{\bar{q}_\sigma^{(j)}\}) \\
&\qquad + \frac{1}{2}\left.\frac{\partial^2 E_\sigma(Q,\{q_j\})}{\partial Q^2}\right|_{Q=\bar{Q}_\sigma}(Q-\bar{Q}_\sigma)^2 \\
&\qquad + \frac{1}{2}\sum_{j=1}^{N}\left.\frac{\partial^2 E_\sigma(Q,\{q_j\})}{\partial q_j^2}\right|_{q_j=\bar{q}_\sigma^j}(q_j-\bar{q}_\sigma^{(j)})^2 \\
&\qquad + \sum_{j=1}^{N}\left.\frac{\partial^2 E_\sigma(Q,\{q_j\})}{\partial Q\partial q_j}\right|_{Q=\bar{Q}_\sigma, q_j=\bar{q}_\sigma^j}(Q-\bar{Q}_\sigma)(q_j-\bar{q}_\sigma^{(j)}). \quad (1)
\end{aligned}
$$

Here we have assumed that the bath modes are not coupled to each other. Within the approximation that the second derivatives with respect to Q and q_j are the same for the reactant and product surfaces, these quantities can be expressed as

$$
\left.\frac{\partial^2 E_\sigma(Q,\{q_j\})}{\partial Q^2}\right|_{Q=\bar{Q}_\sigma} = M\omega_0^2, \qquad \left.\frac{\partial^2 E_\sigma(Q,\{q_j\})}{\partial q_j^2}\right|_{q_j=\bar{q}_\sigma^{(j)}} = m_j\omega_j^2, \quad (2)
$$

where M and m_j are the masses and ω_0 and ω_j are the frequencies associated with the donor-acceptor and bath oscillators, respectively. The coupling constants C_j are defined as

$$
C_j \equiv \left.\frac{\partial^2 E_\sigma(Q,\{q_j\})}{\partial Q\partial q_j}\right|_{Q=\bar{Q}_\sigma, q_j=\bar{q}_\sigma^j}. \quad (3)
$$

Using the definitions given above, the diabatic potential energy surfaces in Eq. (1) can be expressed in terms of bilinearly coupled harmonic oscillators as follows:

$$
\begin{aligned}
E_\sigma(Q,\{q_j\}) &= E_\sigma(\bar{Q}_\sigma,\{\bar{q}_\sigma^{(j)}\}) + \tfrac{1}{2}M\omega_0^2(Q-\bar{Q}_\sigma)^2 \\
&\quad + \tfrac{1}{2}\sum_{j=1}^{N} m_j\omega_j^2(q_j-\bar{q}_\sigma^{(j)})^2 \\
&\quad + \sum_{j=1}^{N} C_j(Q-\bar{Q}_\sigma)(q_j-\bar{q}_\sigma^{(j)}). \quad (4)
\end{aligned}
$$

The last term in Eq. (4) represents the bilinear coupling between the donor-acceptor mode and the bath oscillators. Figure 2 shows the contour plots of the diabatic potential energy surfaces as functions of a single bath mode and the donor-acceptor mode. Note that adding the bilinear coupling term in the form given in Eq. (4) does not affect the equilibrium positions (i.e., the minima) of the surfaces.

In this model, the nonadiabatic coupling V depends explicitly on only the donor-acceptor distance Q. The coupling is independent of the bath coordinates within the Condon approximation, which has been found to be physically reasonable for typical hydrogen tunneling systems.[37] Expanding the logarithm of the coupling in a Taylor series around $Q=(\bar{Q}_R+\bar{Q}_P)/2$ and retaining the terms up to first order lead to the following expression:

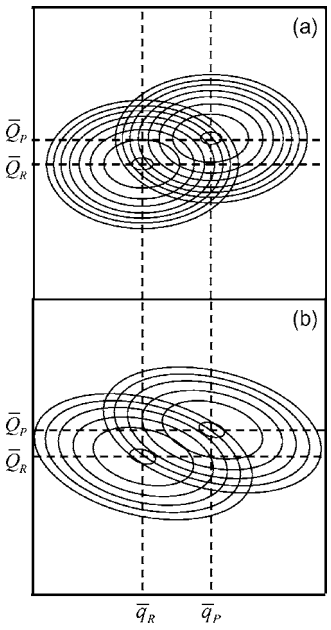

FIG. 2. Contour plots of the reactant and product potential energy surfaces as functions of the donor-acceptor coordinate Q and a bath mode coordinate q. The surfaces are shown for systems with (a) uncoupled donor-acceptor and bath coordinates and (b) coupled donor-acceptor and bath coordinates. Note that the minima of the potential energy surfaces are not affected by the coupling between the coordinates.

$$
V(Q) \approx V_0 \exp[-\alpha Q], \quad (5)
$$

where the origin of the Q coordinate was chosen to be $(\bar{Q}_R+\bar{Q}_P)/2$. This form of the coupling was used previously for nonadiabatic proton transfer systems.[24,26,28] The parameter α determines the distance dependence of the coupling and depends on the specific system. The value of α is typically 25–30 Å^{-1} for intramolecular proton-transfer systems[27] and 10–15 Å^{-1} for proton-coupled electron transfer reactions.[34]

As a result of the bilinear coupling between the bath modes and the Q mode, the simplified picture depicted in Fig. 1 is no longer strictly valid. In particular, the Q mode can slightly impact the relative energies of the two states, and the bath modes can slightly impact the coupling (i.e., the barrier height and width) indirectly through the bilinear coupling. Since the bilinear coupling between the bath modes and the Q mode is typically small relative to the coupling between the bath modes and the TLS, however, Fig. 1 serves as a useful approximate physical picture.

B. Spin-boson Hamiltonian

The spin-boson Hamiltonian corresponding to the TLS coupled to the donor-acceptor mode and the bath oscillators described in the preceding section is

$$
H = -\Delta_0\sigma_z + V_0 e^{-\alpha Q}\sigma_x + H_Q + H_b + H_{Q-b} + \Delta U(Q). \quad (6)
$$

The TLS is represented by the Pauli spin matrices σ_z and σ_x describing a fermionic system. Δ_0 is the energy bias parameter and represents the energy difference between the reactant and product states for the isolated TLS. The Hamiltonians for the donor-acceptor mode and the bath [i.e., the third

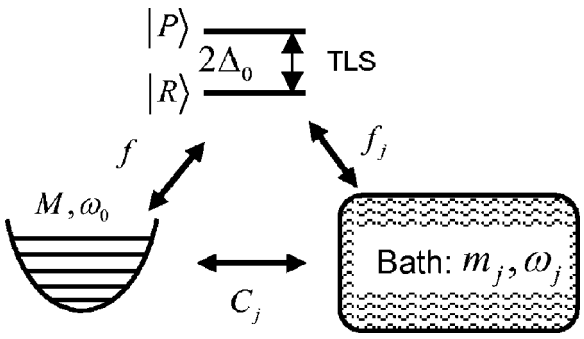

FIG. 3. Schematic diagram of the model for hydrogen tunneling. The three subsystems are the two-level system (TLS) with splitting $2\Delta_0$, the donor-acceptor mode with mass M and frequency ω_0, and the bath consisting of modes with masses m_j and frequencies ω_j. The subsystems are coupled through the coupling constants f, f_j, and C_j.

and fourth terms in Eq. (6), respectively] correspond to shifted harmonic oscillators linearly coupled to the TLS and can be expressed as

$$H_Q = \frac{1}{2}\left\{\frac{P^2}{M} + M\omega_0^2\left(Q + \frac{f\sigma_z}{M\omega_0^2}\right)^2\right\},$$
$$H_b = \frac{1}{2}\sum_{j=1}^{N}\left\{\frac{p_j^2}{m_j} + m_j\omega_j^2\left(q_j + \frac{f_j\sigma_z}{m_j\omega_j^2}\right)^2\right\}, \tag{7}$$

where P and p_j are the conjugate momenta of the coordinates Q and q_j, respectively, and f and f_j are coupling constants. Note that the shifts of the harmonic oscillators arise from the coupling between the TLS and the donor-acceptor and bath oscillators.

The interaction term

$$H_{Q-b} = \sum_{j=1}^{N} C_j\left(Q + \frac{f\sigma_z}{M\omega_0^2}\right)\left(q_j + \frac{f_j\sigma_z}{m_j\omega_j^2}\right) \tag{8}$$

includes the bilinear couplings between the Q mode and the bath oscillators with coupling constants C_j. The coupling constants f_j and C_j can be related to the spectral density functions $\tilde{J}$ and J defined as

$$\tilde{J}(\omega) = \pi\sum_{j=1}^{N}\frac{2f_j^2}{m_j\omega_j}\delta(\omega-\omega_j),$$
$$J(\omega) = \frac{\pi}{2}\sum_{j=1}^{N}\frac{C_j^2}{m_j\omega_j}\delta(\omega-\omega_j). \tag{9}$$

The last term $\Delta U(Q)$ in Eq. (6) is a counterpotential added to avoid the renormalization of the Q-mode frequency ω_0 due to the coupling to the bath. The expression for this term is derived in Appendix A.

Figure 3 provides a diagrammatic depiction of the Hamiltonian given in Eq. (6). This diagram illustrates the possible dissipation mechanisms governing the dynamics of the model system. The three subsystems (TLS, Q mode, and bath) interact with each other through the coupling constants f, f_j, and C_j. When the coupling constants C_j vanish, this Hamiltonian becomes equivalent to the spin-boson Hamiltonian used by Suarez and Silbey.[28] The additional coupling between the Q mode and the bath leads to dispersion of the Q vibration, facilitating the convergence of the time integral of the probability flux correlation function even in the limit of extremely small TLS-bath coupling. The importance of the dispersion of the donor-acceptor mode in proton-transfer reactions has been pointed out previously.[19,28] To our knowledge, however, this dispersion has not been included explicitly within the spin-boson model formalism in previous studies.

For convenience, the Hamiltonian can be rewritten in the second quantization representation with a continuous representation of the bath. The second quantization can be introduced using the standard relations for harmonic oscillators as follows:[38]

$$Q = \sqrt{\frac{\hbar}{2M\omega_0}}(a^\dagger + a), \quad P = i\sqrt{\frac{M\hbar\omega_0}{2}}(a^\dagger - a),$$
$$q_j = \sqrt{\frac{\hbar}{2m_j\omega_j}}(b_j^\dagger + b_j), \quad p_j = i\sqrt{\frac{m_j\hbar\omega_j}{2}}(b_j^\dagger - b_j), \tag{10}$$

where $a^\dagger(a)$ and $b_j^\dagger(b_j)$ are the boson creation (annihilation) operators for the Q oscillator and the jth bath oscillator, respectively. The relationship between the continuous boson operators b_ω and the discretized boson operators b_j is given by[39]

$$b_j = \sqrt{g(\omega_j)}\int_{1/g(\omega_j)} d\omega b_\omega, \tag{11}$$

where $g(\omega)$ is the density of states and $\int_{1/g(\omega_j)}d\omega$ represents the integration over a band of width $1/g(\omega_j)$ around ω_j. The spectral densities defined in Eq. (9) are expressed in the continuous representation as

$$\tilde{J}(\omega) = 2\pi\frac{f_\omega^2 g(\omega)}{m_\omega\omega}, \quad J(\omega) = \frac{\pi}{2}\frac{C_\omega^2 g(\omega)}{m_\omega\omega}. \tag{12}$$

Using the relations in Eq. (10) for the second quantization representation, the transformation in Eq. (11) to a continuous representation of the bath, and Eq. (A6) for the counterpotential term $\Delta U(Q)$, the Hamiltonian in Eq. (6) can be expressed as

$$H = -\Delta_0\sigma_z + V_0\exp\left[-\sqrt{\frac{\lambda_\alpha}{\hbar\omega_0}}(a^\dagger + a)\right]\sigma_x - \frac{\hbar\omega_0}{4}(a^\dagger - a)^2$$
$$+ \frac{M\omega_0^2}{2}\left(\sqrt{\frac{\hbar}{2M\omega_0}}(a^\dagger + a) + \sqrt{\frac{\lambda_Q}{2M\omega_0^2}}\sigma_z\right)^2$$
$$- \int_0^\infty d\omega\frac{\hbar\omega}{4}(b_\omega^\dagger - b_\omega)^2$$
$$+ \int_0^\infty d\omega\frac{m_\omega\omega^2}{2}\left(\sqrt{\frac{\hbar}{2m_\omega\omega}}(b_\omega^\dagger + b_\omega) + \frac{f_\omega\sigma_z}{m_\omega\omega^2}\right.$$
$$\left. + \frac{C_\omega}{m_\omega\omega^2}\left(\sqrt{\frac{\hbar}{2M\omega_0}}(a^\dagger + a) + \sqrt{\frac{\lambda_Q}{2M\omega_0^2}}\sigma_z\right)\right)^2. \tag{13}$$

Here we have introduced the following energy quantities:

$$\lambda_\alpha = \frac{\hbar^2\alpha^2}{2M}, \quad \lambda_Q = \frac{2f^2}{M\omega_0^2}, \tag{14}$$

where λ_Q is the reorganization energy corresponding to the donor-acceptor mode.

C. Nonadiabatic rate constant

In this subsection, we use first-order time-dependent perturbation theory in the form of Fermi's golden rule[38] to calculate the rate constant for nonadiabatic transitions in the system described by the Hamiltonian in Eq. (13). The applicability of this approximation for tunneling reactions has been discussed previously.[12,23,25,26,40–42] In this framework, the total Hamiltonian is partitioned into an unperturbed part and a perturbation. In the case of sufficiently small nonadiabatic coupling, the characteristic relaxation time of the TLS coupled to its environment is much greater than the characteristic relaxation time of the environment. In this case, the perturbation is chosen to be the off-diagonal part of the TLS Hamiltonian proportional to the nonadiabatic coupling V, and the unperturbed Hamiltonian H_0 governs the environmental dynamics

$$H = H_0 + H_1, \tag{15}$$

where

$$\begin{aligned} H_0 &= -\Delta_0\sigma_z + H_Q + H_b + H_{Q-b} + \Delta U(Q), \\ H_1 &= V_0 \exp\left[-\sqrt{\frac{\lambda_\alpha}{\hbar\omega_0}}(a^\dagger + a)\right]\sigma_x. \end{aligned} \tag{16}$$

1. Diagonalization of the unperturbed Hamiltonian

To obtain the eigenstates of H_0, we perform an exact diagonalization procedure in two stages. In the first stage we use the Lang-Firsov unitary transformation,[43] also known as the small polaron transformation,[44] for partial diagonalization. This transformation decouples the fermion spin operators and the boson operators in the unperturbed Hamiltonian by shifting the equilibrium positions of the oscillators. The corresponding operator is chosen to be

$$\begin{aligned} U = \exp\Bigg[&-\frac{\sigma_z}{2}\sqrt{\frac{\lambda_Q}{\hbar\omega_0}}(a^\dagger - a) \\ &-\frac{\sigma_z}{\hbar}\int_0^\infty d\omega f_\omega \sqrt{\frac{\hbar g(\omega)}{2m_\omega\omega^3}}(b_\omega^\dagger - b_\omega)\Bigg]. \end{aligned} \tag{17}$$

Neglecting constant terms, the transformed Hamiltonian is

$$\bar{H} = U^\dagger H U = \bar{H}_0 + \bar{H}_1,$$

$$\begin{aligned} \bar{H}_0 = &-\Delta_0\sigma_z + \hbar\omega_0 a^\dagger a + \int_0^\infty d\omega\hbar\omega b_\omega^\dagger b_\omega \\ &+ \hbar\int_0^\infty d\omega\Bigg[\nu(\omega)(a^\dagger + a)(b_\omega^\dagger + b_\omega) \\ &+ \frac{\nu(\omega)^2}{\omega}(a^\dagger + a)^2\Bigg], \end{aligned} \tag{18}$$

$$\bar{H}_1 = \bar{V}\sigma_x,$$

with

$$\begin{aligned} \bar{V} = V_0 &\exp[(-\Lambda_\alpha + \sigma_z\Lambda_Q)a^\dagger - (\Lambda_\alpha + \sigma_z\Lambda_Q)a] \\ &\times\exp\left[\int_0^\infty d\omega\sigma_z F_\omega(b_\omega^\dagger - b_\omega)\right], \end{aligned} \tag{19}$$

where the dimensionless parameters Λ_α and Λ_Q are defined as

$$\Lambda_\alpha = \sqrt{\frac{\lambda_\alpha}{\hbar\omega_0}}, \quad \Lambda_Q = \sqrt{\frac{\lambda_Q}{\hbar\omega_0}} \tag{20}$$

and

$$\nu(\omega) = \frac{C_\omega}{2}\sqrt{\frac{g(\omega)}{M\omega_0 m_\omega\omega}} = \sqrt{\frac{1}{2\pi}\frac{J(\omega)}{M\omega_0}}, \tag{21}$$

$$F_\omega = \sqrt{\frac{2f_\omega^2 g(\omega)}{\hbar m_\omega\omega^3}} = \frac{1}{\omega}\sqrt{\frac{\tilde{J}(\omega)}{\pi\hbar}}. \tag{22}$$

The transformed unperturbed Hamiltonian describes the TLS in a bath of oscillators that instantaneously adjust their positions to the current state of the TLS. This representation, analogous to the Born-Oppenheimer approximation in electronic structure theory, provides the optimal partition of the total Hamiltonian for the case of strong coupling between the bath and the TLS and relatively high temperatures. In the case of weak coupling or low temperatures, the parameters of this transformation should be variationally optimized to ensure that the dynamics of the unperturbed system is as close as possible to the full system dynamics.[45] Unfortunately, the dynamics emerging for the unperturbed Hamiltonians satisfying the variational principle for the free energy[46] is quite complicated and cannot be treated analytically. Here we assume that the transformed perturbation remains small enough to justify this procedure.

In the second stage of the diagonalization procedure, we perform an exact diagonalization of the bosonic oscillatory part of the Hamiltonian $\bar{H}_0$ following the method introduced by Fano[47] and utilized by Da Costa *et al.* in Ref. 48 for the case of a damped harmonic oscillator. The operators a and b_ω are expanded in terms of new operators A_ω as

$$a = \int_0^\infty d\omega(\alpha_\omega^* A_\omega - \chi_\omega A_\omega^\dagger), \tag{23}$$

$$b_\Omega = \int_0^\infty d\omega(\beta^*_{\omega,\Omega}A_\omega - \sigma_{\omega,\Omega}A^\dagger_\omega). \tag{24}$$

The coefficients are determined by imposing a commutation relation

$$[A_\omega, \bar{H}_0] = \hbar\omega A_\omega \tag{25}$$

to ensure that $\bar{H}_0$ is diagonalized. The resulting coefficients are[48]

$$|\alpha_\omega|^2 = \left(\frac{\omega+\omega_0}{2\omega_0}\right)^2 \frac{1}{\nu(\omega)^2[\pi^2 + z^2(\omega)]}, \tag{26}$$

$$\chi_\omega = \frac{\omega-\omega_0}{\omega+\omega_0}\alpha_\omega, \tag{27}$$

$$\beta_{\omega,\Omega} = \left[\mathcal{P}\frac{1}{\omega-\Omega} + z(\omega)\delta(\omega-\Omega)\right]\frac{2\omega_0}{\omega+\omega_0}\nu(\Omega)\alpha_\omega, \tag{28}$$

$$\sigma_{\omega,\Omega} = \frac{1}{\omega+\Omega}\frac{2\omega_0}{\omega+\omega_0}\nu(\Omega)\alpha_\omega, \tag{29}$$

where

$$z(\omega) = \frac{\omega^2 - \omega_0^2 - 2\omega_0 H_R(\omega)}{2\omega_0\nu(\omega)^2}, \tag{30}$$

$$H_R(\omega) = \mathcal{P}\int_0^\infty \frac{\nu(\Omega)^2}{\omega-\Omega}d\Omega - \int_0^\infty \frac{\nu(\Omega)^2}{\omega+\Omega}d\Omega + 2\int_0^\infty \frac{\nu(\Omega)^2}{\Omega}d\Omega, \tag{31}$$

and $\mathcal{P}$ denotes the Cauchy principal value of the integral.

The resulting transformed unperturbed Hamiltonian in terms of the new boson operators A_ω acquires the following simple form:

$$\tilde{H}_0 = -\Delta_0\sigma_z + \int_0^\infty d\omega\hbar\omega A^\dagger_\omega A_\omega = -\Delta_0\sigma_z + \tilde{H}_A. \tag{32}$$

Note that the new boson operators A_ω correspond to normal modes of the environment that are combinations of the bath modes and the donor-acceptor mode and are not coupled to each other within the unperturbed Hamiltonian.

The transformed perturbation is $\tilde{H}_1 = \tilde{V}\sigma_x$, where

$$\tilde{V} = V_0 \exp\left[\int_0^\infty d\omega[-\alpha^*_\omega(\Lambda_\alpha + \sigma_z\Lambda_Q) + \chi^*_\omega(\Lambda_\alpha - \sigma_z\Lambda_Q)]A_\omega\right]\exp\left[\int_0^\infty d\omega[-\alpha_\omega(\Lambda_\alpha - \sigma_z\Lambda_Q) + \chi_\omega(\Lambda_\alpha + \sigma_z\Lambda_Q)]A^\dagger_\omega\right] \times\exp\left[\int_0^\infty d\omega\int_0^\infty d\Omega\sigma_z F_\Omega[-(\beta^*_{\omega,\Omega} + \sigma^*_{\omega,\Omega})A_\omega + (\beta_{\omega,\Omega} + \sigma_{\omega,\Omega})A^\dagger_\omega]\right]. \tag{33}$$

The thermal average of the transformed perturbation matrix element is

$$\langle\tilde{V}\rangle = \exp\left[\int_0^\infty d\omega\left\{\frac{\lambda_\alpha}{\hbar\omega_0} - \frac{\omega^2}{\omega_0^2}\frac{\lambda_Q}{\hbar\omega_0} - 2\sqrt{\frac{\lambda_Q}{\hbar\omega_0}}\frac{\omega}{\omega_0}[\kappa(\omega)+\Pi(\omega)] + \frac{\tilde{J}(\omega)J(\omega)}{2\hbar\omega_0\omega^2 M} - \Pi(\omega)^2 - 2\Pi(\omega)\kappa(\omega)\right\}\xi(\omega)L(\omega)\right] \times\exp\left[-\frac{1}{\hbar\pi}\int_0^\infty d\omega\xi(\omega)\frac{\tilde{J}(\omega)}{\omega^2}\right], \tag{34}$$

where the last term represents the thermal average of the Franck-Condon factor for the displaced bath oscillators. Here $\langle(\cdots)\rangle$ denotes the thermal average over the eigenstates of $\tilde{H}_A$ (i.e., the quantum states of the environment),

$$\langle(\cdots)\rangle = \frac{\mathrm{Tr}[(\cdots)e^{-\beta\tilde{H}_A}]}{\mathrm{Tr}[e^{-\beta\tilde{H}_A}]} \tag{35}$$

and

$$\xi(\omega) = \coth\left(\frac{\beta\hbar\omega}{2}\right), \tag{36}$$

$$L(\omega) = \frac{(2\omega_0/\pi)(J(\omega)/M)}{(J(\omega)/M)^2 + (\omega^2 - \omega_0^2 - 2\omega_0 H_R(\omega))^2}, \tag{37}$$

$$\kappa(\omega) = \frac{1}{\omega}\sqrt{\frac{M}{2\hbar\omega_0}\frac{\tilde{J}(\omega)}{J(\omega)}}(\omega^2 - \omega_0^2 - 2\omega_0 H_R(\omega)), \tag{38}$$

$$\Pi(\omega) = \sqrt{\frac{1}{2\pi^2\hbar\omega_0 M}}\left(\mathcal{P}\int_0^\infty d\Omega\frac{1}{\Omega}\frac{\sqrt{\tilde{J}(\Omega)J(\Omega)}}{(\omega-\Omega)} + \int_0^\infty d\Omega\frac{1}{\Omega}\frac{\sqrt{\tilde{J}(\Omega)J(\Omega)}}{(\omega+\Omega)}\right). \tag{39}$$

The magnitude of $\langle\tilde{V}\rangle$ depends on the choice of the spectral densities. For spectral densities of the form $\tilde{J}(\omega) \propto \omega^s f_c(\omega)$, where $f_c(\omega)$ is a frequency cut-off function, $\langle\tilde{V}\rangle = 0$ for $s < 3$ due to the divergence of the integral in the last

exponential of Eq. (34) at $\omega \to +0$. This phenomenon, usually referred to as the infrared divergence, is well known in the spin-boson problem[49] and determines the qualitative aspects of the dynamics of the TLS coupled to the dissipative environment. In the case of $\langle \tilde{V} \rangle = 0$, the dynamics of the tunneling transitions are purely incoherent, i.e., the transitions are induced solely by the thermal fluctuations of the environmental degrees of freedom. At zero temperature in this regime, the dynamics are fully suppressed and the tunneling particle remains in the initial localized state, yielding zero rate constant in first-order perturbation theory. At finite temperatures, the golden rule rate constant can be defined provided that dissipative channels are available.

In the present work, we use Ohmic spectral densities ($s=1$), which are considered to be relevant to chemical reactions in disordered media such as solution and protein environments.[50] The use of Ohmic spectral densities could be viewed as an approximation made for the purposes of analytic simplification. Nevertheless, we expect that the use of the mathematically simple Ohmic form will enable us to capture the most significant qualitative features of energy dissipation in our model. As mentioned above, the thermal average of the coupling vanishes (i.e., $\langle \tilde{V} \rangle = 0$) for Ohmic spectral densities. This property ensures that the correlation function required for the calculation of the golden rule rate constant approaches zero at infinite time.

2. Derivation of rate constant for nonadiabatic quantum transitions

Since the Hamiltonian $\tilde{H}_A$ is not coupled to the TLS, the initial and final states for the hydrogen tunneling reaction in the basis of eigenstates of the unperturbed Hamiltonian can be expressed as direct products $|R\rangle|m\rangle$ and $|P\rangle|n\rangle$, respectively, where $|m\rangle$ and $|n\rangle$ are the eigenstates of $\tilde{H}_A$ with associated eigenvalues ε_m and ε_n, respectively. The energies of the initial and final states $|R\rangle|m\rangle$ and $|P\rangle|n\rangle$ are $E_{Rm} = -\Delta_0 + \varepsilon_m$ and $E_{Pn} = \Delta_0 + \varepsilon_n$, respectively.

The golden rule rate constant for quantum transitions from the manifold $|R\rangle|m\rangle$ to the manifold $|P\rangle|n\rangle$ is

$$\begin{aligned} k &= \frac{2\pi}{\hbar} \sum_m \sum_n P_{Rm} \langle m | \langle R | \tilde{V} \sigma_x | P \rangle | n \rangle \\ &\quad \times \langle n | \langle P | \tilde{V} \sigma_x | R \rangle | m \rangle \delta(E_{Pn} - E_{Rm}) \\ &= \frac{1}{\hbar^2} \int_{-\infty}^{\infty} dt \sum_m \sum_n P_{Rm} \langle m | \tilde{V}_{RP} | n \rangle \\ &\quad \times \langle n | e^{(i/\hbar)\tilde{H}_A t} \tilde{V}_{PR} e^{-(i/\hbar)\tilde{H}_A t} | m \rangle e^{i2\Delta_0 t} \\ &= \frac{1}{\hbar^2} \int_{-\infty}^{\infty} dt \sum_m \sum_n P_{Rm} \langle m | \tilde{V}_{RP} | n \rangle \langle n | \tilde{V}_{PR}(t) | m \rangle e^{i2\Delta_0 t} \\ &= \frac{1}{\hbar^2} \int_{-\infty}^{\infty} dt j(t), \end{aligned} \tag{40}$$

where the summations are over eigenstates of $\tilde{H}_A$, and the Boltzmann probability P_{Rm} for the initial state $|R\rangle|m\rangle$ is

$$P_{Rm} = \frac{e^{-\beta \varepsilon_m}}{\mathrm{Tr}[e^{-\beta \tilde{H}_A}]}. \tag{41}$$

The probability flux correlation function $j(t)$ is

$$j(t) = e^{i2\Delta_0 t} \langle \tilde{V}_{RP} \tilde{V}_{PR}(t) \rangle, \tag{42}$$

where $\langle (\cdots) \rangle$ denotes the thermal average over quantum states of the environment, as defined in Eq. (35). The transition matrix elements between $|R\rangle$ and $|P\rangle$ are

$$\begin{aligned} \tilde{V}_{RP} &= \langle R | \tilde{V} \sigma_x | P \rangle \\ &= V_0 \exp\left[\int_0^{\infty} d\omega \{\theta_1(\omega) - \Phi(\omega)\} A_\omega \right. \\ &\quad \left. + \{\theta_2(\omega) + \Phi^*(\omega)\} A_\omega^\dagger \right], \\ \tilde{V}_{PR} &= \langle P | \tilde{V} \sigma_x | R \rangle \\ &= V_0 \exp\left[\int_0^{\infty} d\omega \{\theta_2^*(\omega) + \Phi(\omega)\} A_\omega \right. \\ &\quad \left. + \{\theta_1^*(\omega) - \Phi^*(\omega)\} A_\omega^\dagger \right], \end{aligned} \tag{43}$$

where

$$\begin{aligned} \theta_1(\omega) &\equiv -(\Lambda_\alpha + \Lambda_Q)\alpha_\omega^* + (\Lambda_\alpha - \Lambda_Q)\chi_\omega^*, \\ \theta_2(\omega) &\equiv -(\Lambda_\alpha - \Lambda_Q)\alpha_\omega + (\Lambda_\alpha + \Lambda_Q)\chi_\omega, \\ \Phi(\omega) &\equiv \int_0^{\infty} d\Omega F_\Omega (\beta_{\omega,\Omega}^* + \sigma_{\omega,\Omega}^*). \end{aligned} \tag{44}$$

Evaluating the thermal average $\langle \tilde{V}_{RP} \tilde{V}_{PR}(t) \rangle$ in Eq. (42) leads to the following expression for the probability flux correlation function:

$$j(t) = |V_0|^2 e^{i2\Delta_0 t} \exp[\Phi_Q(t) + \Phi_b(t) + \Phi_{Q-b}(t)]. \tag{45}$$

The expressions for the three terms are given below. All of these terms involve the quantum oscillatory quantities defined by

$$\begin{aligned} \zeta(\omega,t) &= \xi(\omega)\cos\omega t + i \sin\omega t, \\ \tilde{\zeta}(\omega,t) &= \cos\omega t + i\xi(\omega)\sin\omega t. \end{aligned} \tag{46}$$

The first term in the exponential in Eq. (45) is

$$\begin{aligned} \Phi_Q(t) = \int_0^{\infty} d\omega \left\{ \frac{\lambda_\alpha}{\hbar\omega_0} [\zeta(\omega,t) + \xi(\omega)] \right. \\ + \left(\frac{\omega}{\omega_0} \right)^2 \frac{\lambda_Q}{\hbar\omega_0} [\zeta(\omega,t) - \xi(\omega)] \\ \left. + 2\frac{\sqrt{\lambda_\alpha \lambda_Q}}{\hbar\omega_0} \frac{\omega}{\omega_0} \tilde{\zeta}(\omega,t) \right\} L(\omega). \end{aligned} \tag{47}$$

This term represents contributions from the dynamics of the donor-acceptor mode. Note that this term does not vanish

even in the absence of explicit coupling between the TLS and the Q mode (i.e., when the Q-mode reorganization energy $\lambda_Q=0$). In this case, the contributions to this term arise from λ_α, which reflects the dependence of the nonadiabatic coupling V on the donor-acceptor distance Q.

The second term depends on the spectrum of the interactions between the bath and the TLS,

$$\Phi_b(t)=\frac{1}{\pi\hbar}\int_0^\infty d\omega[\zeta(\omega,t)-\xi(\omega)]\frac{\tilde{J}(\omega)}{\omega^2}. \tag{48}$$

This term describes the damping effects of the bath arising from the energy dissipation channel between the TLS and the bath characterized by the bath reorganization energy λ_b,

$$\lambda_b=\frac{1}{\pi}\int_0^\infty d\omega\frac{\tilde{J}(\omega)}{\omega}. \tag{49}$$

When the bath is not explicitly coupled to the TLS, $\tilde{J}(\omega)=0$ and the corresponding bath reorganization energy is zero. In this case, the term defined in Eq. (48) vanishes.

The third term describes the dynamical interference effects between the donor-acceptor motion and the bath thermal fluctuations,

$$\begin{aligned}\Phi_{Q-b}(t)=\int_0^\infty d\omega 2\Bigg\{&\sqrt{\frac{\lambda_\alpha}{\hbar\omega_0}}[\kappa(\omega)\zeta(\omega,t)+\tilde{\zeta}(\omega,t)\Pi(\omega)]\\&+\Bigg[\sqrt{\frac{\lambda_Q}{\hbar\omega_0}}\frac{\omega}{\omega_0}[\kappa(\omega)+\Pi(\omega)]+\kappa(\omega)\Pi(\omega)\\&+\frac{1}{2}\Bigg[\Pi(\omega)^2-\frac{\tilde{J}(\omega)J(\omega)}{2\hbar\omega_0\omega^2M}\Bigg]\Bigg]\\&\times[\zeta(\omega,t)-\xi(\omega)]\Bigg\}L(\omega),\end{aligned} \tag{50}$$

where $\kappa(\omega)$ and $\Pi(\omega)$ are defined in Eqs. (38) and (39), respectively. This term vanishes when the bath is not directly coupled to the TLS [i.e., when $\tilde{J}(\omega)=0$] or the bath is not directly coupled to the Q mode [i.e., when $J(\omega)=0$], but it can be nonzero even if the Q mode is not coupled to the TLS (i.e., $\lambda_Q=0$).

3. Probability flux correlation function for Ohmic dissipation

For the remaining derivations, we use Ohmic spectral densities with Drude-type cutoffs

$$\tilde{J}(\omega)=\eta\omega\frac{\tilde{\Omega}_c^2}{\tilde{\Omega}_c^2+\omega^2},\quad J(\omega)=M\gamma\omega\frac{\Omega_c^2}{\Omega_c^2+\omega^2}, \tag{51}$$

where $\tilde{\Omega}_c$ and Ω_c are the corresponding cut-off frequencies. Here η is the friction coefficient corresponding to the coupling between the bath and the TLS, and γ is the friction constant corresponding to the coupling between the bath and the Q mode. Using the sum rule in Eq. (49), we can establish the relationship between the friction coefficient η and the bath reorganization energy λ_b

$$\eta=\frac{2\lambda_b}{\tilde{\Omega}_c}. \tag{52}$$

For the spectral densities given in Eq. (51), the frequency shift $H_R(\omega)$ defined in Eq. (31) can be evaluated analytically to be

$$H_R(\omega)=\frac{1}{2}\frac{\gamma\Omega_c}{\omega_0}\frac{\omega^2}{\omega^2+\Omega_c^2}. \tag{53}$$

When $\Omega_c\gg\omega_0$, $H_R(\omega)\approx 0$ for $\omega\approx\omega_0$. Since the function $L(\omega)$ is sharply peaked around $\omega\approx\omega_0$ for $\gamma\ll\omega_0$, $H_R(\omega)$ can be neglected for the remainder of the derivation.[48]

The integration over frequencies in Eqs. (47), (48), and (50) can be performed analytically using the contour integration technique (see Appendix B). The full analytic expression for $\Phi_Q(t)$ includes three terms as follows:

$$\Phi_Q(t)=\Phi_Q^L(t)+\Phi_Q^M(t)+\Phi_Q^N(t). \tag{54}$$

The first term $\Phi_Q^L(t)$ originates from the dynamics of the damped Q-mode oscillator representing the donor-acceptor mode coupled to the bath and is expressed as

$$\begin{aligned}\Phi_Q^L(t)=&\frac{\lambda_\alpha}{2\hbar\bar{\omega}}e^{-(\gamma/2)t}\{e^{i\bar{\omega}t}[\xi(\omega_+)+1]-e^{-i\bar{\omega}t}[\xi(\omega_-)+1]+\xi(\omega_+)-\xi(\omega_-)\}+\frac{\lambda_Q}{2\hbar\bar{\omega}}e^{-(\gamma/2)t}\Bigg\{\frac{\omega_+^2}{\omega_0^2}[e^{i\bar{\omega}t}[\xi(\omega_+)+1]-\xi(\omega_+)]\\&-\frac{\omega_-^2}{\omega_0^2}[e^{-i\bar{\omega}t}[\xi(\omega_-)+1]-\xi(\omega_-)]\Bigg\}+\frac{\sqrt{\lambda_\alpha\lambda_Q}}{\hbar\bar{\omega}}e^{-(\gamma/2t)}\Bigg\{\frac{\omega_+}{\omega_0}e^{i\bar{\omega}t}[\xi(\omega_+)+1]-\frac{\omega_-}{\omega_0}e^{-i\bar{\omega}t}[\xi(\omega_-)+1]\Bigg\},\end{aligned} \tag{55}$$

where

$$\bar{\omega}=\sqrt{\omega_0^2-\frac{\gamma^2}{4}},\quad \omega_+=\bar{\omega}+i\frac{\gamma}{2},\quad \omega_-=-\bar{\omega}+i\frac{\gamma}{2}. \tag{56}$$

Note that the exponential factor $e^{-(\gamma/2)}$ damps the oscillations. The second term $\Phi_Q^M(t)$ represents the contributions from the Matsubara frequencies,

$$\Phi_Q^M(t) = -\frac{4\gamma}{\beta\hbar^2}\sum_{n=1}^{\infty}\frac{D(i\nu_n)\nu_n}{(\nu_n^2+\omega_0^2)^2-\gamma^2\nu_n^2}\left[\lambda_\alpha(1+e^{-\nu_n t}) + \lambda_Q(1-e^{-\nu_n t})\frac{\nu_n^2}{\omega_0^2} + 2i\sqrt{\lambda_\alpha\lambda_Q}e^{-\nu_n t}\frac{\nu_n}{\omega_0}\right], \tag{57}$$

where the Matsubara frequencies are defined as $\nu_n = 2\pi n/\beta\hbar$ and

$$D(i\nu_n) = \frac{\Omega_c^2}{\Omega_c^2-\nu_n^2}. \tag{58}$$

The last term $\Phi_Q^N(t)$ is specific to the Drude form of the cut-off function and is given by

$$\Phi_Q^N(t) = \frac{i\gamma\Omega_c^2}{-\gamma^2\Omega_c^2+(\Omega_c^2+\omega_0^2)^2}\left[\xi(i\Omega_c)\left(\frac{\lambda_\alpha}{\hbar}+\frac{\lambda_Q}{\hbar}\frac{\Omega_c^2}{\omega_0^2}\right) + (\xi(i\Omega_c)+1)\left(\sqrt{\frac{\lambda_\alpha}{\hbar}}+i\sqrt{\frac{\lambda_Q}{\hbar}}\frac{\Omega_c}{\omega_0}\right)^2 e^{-\Omega_c t}\right]. \tag{59}$$

The interference term $\Phi_{Q-b}(t)$ is given by the following expression:

$$\Phi_{Q-b}(t) = \Phi_{Q-b}^{\alpha}(t) + \Phi_{Q-b}^{Q}(t), \tag{60}$$

where

$$\Phi_{Q-b}^{\alpha}(t) = \frac{1}{\hbar\bar{\omega}}\sqrt{\frac{\lambda_\alpha\lambda_b\gamma}{\tilde{\Omega}_c}}\left[e^{i\omega_+ t}[\xi(\omega_+)+1]G(\omega_+) - e^{i\omega_- t}[\xi(\omega_-)+1]G(\omega_-) - 2\bar{\omega}\bar{\Omega}_c e^{-\bar{\Omega}_c t}[1+\xi(i\bar{\Omega}_c)]\frac{\omega_0^2+\bar{\Omega}_c^2+\gamma\bar{\Omega}_c}{-\gamma^2\bar{\Omega}_c^2+(\bar{\Omega}_c^2+\omega_0^2)^2} - i\frac{4\bar{\omega}}{\beta\hbar\omega_0^2}\right] \tag{61}$$

and

$$\Phi_{Q-b}^{Q}(t) = \frac{1}{\hbar\bar{\omega}}\sqrt{\frac{\lambda_Q\lambda_b\gamma}{\tilde{\Omega}_c}}\left[\{e^{i\omega_+ t}[\xi(\omega_+)+1]-\xi(\omega_+)\}\frac{\omega_+}{\omega_0}G(\omega_+) - \{e^{i\omega_- t}[\xi(\omega_-)+1]-\xi(\omega_-)\}\frac{\omega_-}{\omega_0}G(\omega_-) - i\frac{\bar{\omega}}{\omega_0}\frac{2\bar{\Omega}_c^2}{\gamma^2\bar{\Omega}_c^2-(\bar{\Omega}_c^2+\omega_0^2)^2}[(1-e^{-\bar{\Omega}_c t})\{\gamma\bar{\Omega}_c+\xi(i\bar{\Omega}_c)(\bar{\Omega}_c^2+\omega_0^2+\gamma\bar{\Omega}_c)\}-(\bar{\Omega}_c^2+\omega_0^2)e^{-\bar{\Omega}_c t}]\right], \tag{62}$$

with

$$G(\omega) = \Pi_0(\omega) + i\bar{D}(\omega), \tag{63}$$

$$\bar{D}(\omega) = \frac{\bar{\Omega}_c^2}{\bar{\Omega}_c^2+\omega^2}. \tag{64}$$

The reduced cut-off frequency $\bar{\Omega}_c$ for the geometrical mean of the spectral densities $\bar{J}(\omega)=\sqrt{\tilde{J}(\omega)J(\omega)}$ is defined as

$$\bar{\Omega}_c = \frac{2\tilde{\Omega}_c\Omega_c}{\tilde{\Omega}_c+\Omega_c}. \tag{65}$$

The bath contribution $\exp[\Phi_b(t)]$ describes the damping effect originating from thermal fluctuations of the bath. The approximate analytic expression obtained in the high-temperature limit for the bath modes, where $\beta\hbar\tilde{\Omega}_c \ll 1$, is

$$\exp[\Phi_b(t)] = \exp\left[\frac{2\lambda_b}{\beta\hbar^2\tilde{\Omega}_c^2}(1-e^{-\tilde{\Omega}_c t}-\tilde{\Omega}_c t) + i\frac{\lambda_b}{\hbar\tilde{\Omega}_c}(1-e^{-\tilde{\Omega}_c t})\right]. \tag{66}$$

This term can be simplified in two different limits depending on the parameter Λ,[40]

$$\Lambda = \sqrt{\frac{2\lambda_b}{\beta\hbar^2\tilde{\Omega}_c^2}}. \tag{67}$$

The strong solvation regime corresponds to relatively large bath reorganization energies (i.e., $\Lambda \gg 1$). Using a short-time approximation [i.e., expanding the exponentials in the exponent of Eq. (66) to second order], we obtain the following expression for the bath contribution, which exhibits Gaussian damping behavior:

$$\exp[\Phi_b(t)] \approx \exp\left[-\frac{\lambda_b}{\beta\hbar^2}t^2 + i\left(\frac{\lambda_b}{\hbar}t - \frac{\tilde{\Omega}_c\lambda_b}{2\hbar}t^2\right)\right]. \tag{68}$$

The weak solvation regime corresponds to relatively small bath reorganization energies (i.e., $\Lambda \ll 1$). In this limit, $\exp[\Phi_b(t)]$ decays very slowly, and the linear term $-\tilde{\Omega}_c t$ in

the exponent of Eq. (66) becomes dominant. Neglecting the contributions of $1-e^{-\tilde{\Omega}_c t}$ in the exponent, we obtain

$$\exp[\Phi_b(t)] \approx \exp\left[-\frac{2\lambda_b}{\beta\hbar^2\tilde{\Omega}_c}t\right]. \tag{69}$$

In the limit of $\gamma \to 0$ the expression for the probability flux correlation function given in Eq. (45) reduces to the expression derived by Suarez and Silbey[28] in the absence of the coupling between the donor-acceptor mode and the bath. In this limit $\Phi_{Q-b}(t)=0$ and

$$\begin{aligned}\lim_{\gamma\to 0}\Phi_Q(t) = &\frac{\lambda_\alpha}{\hbar\omega_0}[\xi(\omega_0)(\cos\omega_0 t+1)+i\sin\omega_0 t]\\ &+\frac{\lambda_Q}{\hbar\omega_0}[\xi(\omega_0)(\cos\omega_0 t-1)+i\sin\omega_0 t]\\ &+\frac{2\sqrt{\lambda_\alpha\lambda_Q}}{\hbar\omega_0}[\cos\omega_0 t+i\xi(\omega_0)\sin\omega_0 t],\end{aligned} \tag{70}$$

where we used the relations

$$\lim_{\gamma\to 0}\bar{\omega}=\omega_0, \quad \lim_{\gamma\to 0}\xi(\omega_\pm)=\pm\xi(\omega_0). \tag{71}$$

Equation (70) is equivalent to the Q-oscillator part of Eq. (12) in Ref. 28.

III. MODEL CALCULATIONS

In this section we discuss the behavior of the probability flux correlation function in the strong and weak solvation regimes and present the numerical results for the rate constant, as well as its dependence on the temperature T, the energy bias parameter Δ_0, the donor-acceptor mode frequency ω_0, and the friction constant γ corresponding to the coupling between the donor-acceptor mode and the bath.

The value chosen for the bath cut-off frequency $\tilde{\Omega}_c = 100\ \mathrm{cm}^{-1}$ corresponds to the high-temperature limit for the bath modes at room temperature ($\beta\hbar\tilde{\Omega}_c < 1$ at 300 K) and characterizes the translational, librational, and rotational degrees of freedom of the solvent or protein environment. The cut-off frequency Ω_c for the interaction between the donor-acceptor mode and the bath is chosen to be $5000\ \mathrm{cm}^{-1}$ to model the donor-acceptor mode as a damped oscillator following non-Markovian dynamics with short-time memory effects. This cut-off frequency is assumed to be much higher than any of the characteristic frequencies of the environment and is required mainly to ensure convergence of the integrals involving the corresponding spectral density $J(\omega)$.[50]

The donor-acceptor mode reorganization energy λ_Q was calculated with the simple expression for two displaced harmonic potentials

$$\lambda_Q = \tfrac{1}{2}M\omega_0^2\delta Q^2. \tag{72}$$

Here M is the reduced mass of the Q oscillator and was chosen to be 25 amu unless otherwise specified. The parameter δQ is the shift of the equilibrium position $\delta Q = \bar{Q}_P - \bar{Q}_R$ and was chosen to be 0.1 Å. The donor-acceptor mode frequency was $\omega_0 = 70\ \mathrm{cm}^{-1}$ and the temperature was $T = 300$ K unless otherwise specified. The bath reorganization energy was $\lambda_b = 20$ kcal/mol for the strong solvation regime and $\lambda_b = 0.001$ kcal/mol for the weak solvation regime. The nonadiabatic coupling parameters were chosen to be $V_0 = 0.001$ kcal/mol and $\alpha = 15\ \text{Å}^{-1}$.

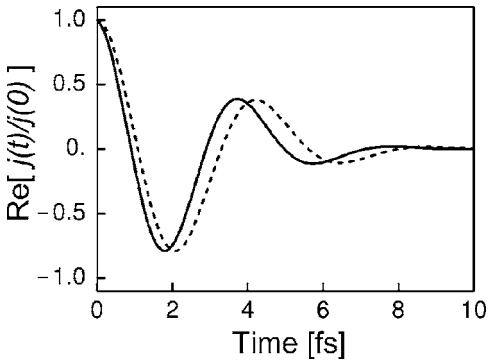

FIG. 4. Probability flux correlation function in the strong solvation regime with $\lambda_b = 20$ kcal/mol and $\Delta_0 = -15$ kcal/mol. The friction constants corresponding to the coupling between the donor-acceptor mode and the bath are $\gamma = 0$ (dashed line) and $\gamma = 20\ \mathrm{cm}^{-1}$ (solid line). The donor-acceptor mode frequency is $\omega_0 = 70\ \mathrm{cm}^{-1}$ and the temperature is $T = 300$ K.

A. Strong solvation regime

In the strong solvation regime, when the parameter Λ defined in Eq. (67) satisfies the condition $\Lambda \gg 1$, the expression for the probability flux correlation function can be simplified. In this case, the terms Φ_Q^M and Φ_Q^N are significantly smaller than the term Φ_Q^L and can be neglected. Thus, the simplified probability flux correlation function is

$$j(t) = |V_0|^2 e^{i2\Delta_0 t}\exp[\Phi_Q^L(t)+\Phi_{Q-b}(t)+\Phi_b(t)], \tag{73}$$

where the solvent damping term $\Phi_b(t)$ is given by Eq. (68). Note that the contribution of the interference term $\Phi_{Q-b}(t)$ was found to be significant for describing the dependence of the rate constant on the friction constant γ and cannot be neglected. In this regime, we can use the short-time approximation and evaluate the time integral analytically using the stationary phase approximation. Unfortunately, the presence of the term $\Phi_{Q-b}(t)$ leads to expressions that are too cumbersome to analyze. Thus, the rate constants presented below were obtained by numerical integration of the probability flux correlation function given in Eq. (73).

The time evolution of the probability flux correlation function for the strong solvation regime is shown in Fig. 4. The probability flux correlation function decays rapidly on the time scale of ~10 fs, exhibiting strong damped behavior that arises from the leading Gaussian decay factor in the term $\exp[\Phi_b(t)]$ given in Eq. (68). As observed previously for model proton-coupled electron transfer reactions with large solvent reorganization energies,[33] in this regime the decay time is determined mainly by the time scale of the bath relaxation, and the dissipation of energy occurs predominantly via the TLS-bath coupling channel. Note that the friction constant γ corresponding to the coupling between the donor-acceptor mode and the bath impacts the quantitative but not the qualitative behavior of the probability flux correlation function.

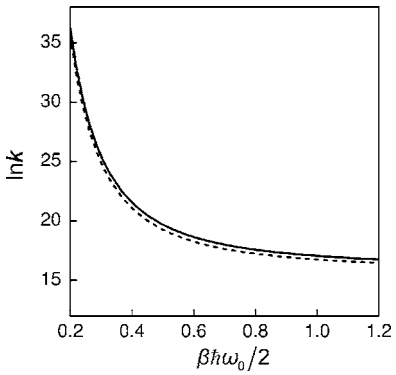

FIG. 5. Dependence of the rate on $\beta\hbar\omega_0/2$ in the strong solvation regime with $\lambda_b=20$ kcal/mol and $\Delta_0=-15$ kcal/mol. The friction constants corresponding to the coupling between the donor-acceptor mode and the bath are $\gamma=0$ (dashed line) and $\gamma=20$ cm^{-1} (solid line). The temperature is $T=300$ K and the donor-acceptor mode frequency ω_0 is varied.

The dependence of the rate constant on the donor-acceptor mode frequency ω_0 is depicted in Fig. 5. The frequency dependence of the rate shows two distinct regions corresponding to the classical or high-temperature ($\beta\hbar\omega_0 \ll 1$) and the quantum or low-temperature ($\beta\hbar\omega_0 \gg 1$) limits for the donor-acceptor vibration. The noticeable enhancement of the rate in the lower frequency region can be attributed to the dependence of the nonadiabatic coupling on the donor-acceptor distance (i.e., the nonadiabatic coupling increases as the donor-acceptor distance decreases). The lower frequency donor-acceptor vibrations enable more effective sampling of the smaller donor-acceptor distances, thereby facilitating the nonadiabatic transitions and increasing the rate constant. Again, the friction constant γ impacts the quantitative but not the qualitative dependence of the rate constant on the frequency of the donor-acceptor mode.

Due to the dominance of the direct TLS-bath energy exchange mechanism in the strong solvation regime, the reaction is a thermally activated process, and the effects of the coupling between the donor-acceptor mode and the bath on the rate constant are very subtle. The dependence of the rate constant on the friction constant γ can be qualitatively different depending on the energy bias parameter Δ_0, which characterizes the asymmetry of the isolated TLS. Figure 6

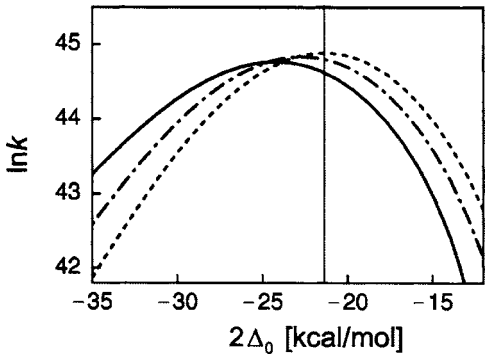

FIG. 6. Dependence of the rate constant on the energy bias $2\Delta_0$ in the strong solvation regime with $\lambda_b=20$ kcal/mol, $\omega_0=70$ cm^{-1}, and $T=300$ K. The dashed, dot-dashed, and solid lines correspond to $\gamma=0$, $\gamma=5$ cm^{-1}, and $\gamma=20$ cm^{-1}, respectively. The thin vertical line separates the inverted regime (left) and the normal regime (right) for $\gamma=0$.

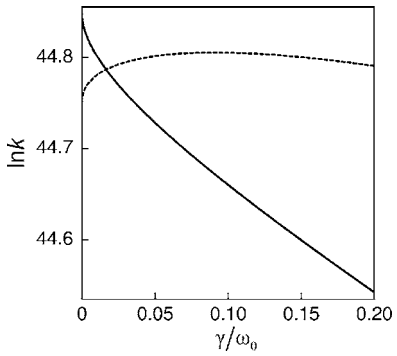

FIG. 7. Dependence of the rate on γ/ω_0 in the strong solvation regime with $\lambda_b=20$ kcal/mol, $\omega_0=70$ cm^{-1}, and $T=300$ K. The dashed and solid lines correspond to $2\Delta_0=-24.0$ kcal/mol (inverted regime) and $2\Delta_0=-20.0$ kcal/mol (normal regime), respectively.

depicts the dependence of the rate constant on the energy bias $2\Delta_0$ for three different values of γ. The maximum of the slightly asymmetric inverted parabola shifts toward more negative values of Δ_0 as γ increases. This shift arises mainly from the dynamical interference term $\Phi_{Q-b}(t)$ given in Eqs. (60)–(62). The physical basis for this shift can be understood in the framework of the standard Marcus model for thermally activated nonadiabatic processes,[15] where the activation free energy of the reaction is approximated as $\Delta G^{\neq}=(\Delta G+\lambda)^2/4\lambda$ for a reaction with an effective total reorganization energy λ and driving force ΔG. The shift of the inverted parabolas with increasing γ in our calculations is associated with the increase of the effective total reorganization energy with γ. According to the Marcus model, the rate constant will exhibit a maximum as a function of γ for values of Δ_0 in the inverted regime and will decrease with γ for values of Δ_0 in the normal regime of the inverted parabola corresponding to $\gamma=0$. This trend is illustrated in Fig. 7, which depicts the dependence of the rate constant on γ for two different values of the energy bias parameter corresponding to the inverted and normal regimes. Note that these phenomena arise from the additional energy exchange channel between the TLS and the bath mediated by the donor-acceptor mode. In the case of a high-frequency donor-acceptor mode (i.e., $\beta\hbar\omega_0 \gg 1$) frozen predominantly in the ground state or $\lambda_Q=0$, this channel is not effective, and the dependence of the rate constant on γ is significantly weaker.

B. Weak solvation regime

In the weak solvation regime ($\Lambda \ll 1$), the dynamical interference term Φ_{Q-b} is significantly smaller than Φ_Q and can be neglected in Eq. (45). In this case, the probability flux correlation function can be simplified as

$$j(t) = |V_0|^2 e^{i2\Delta_0 t} \exp[\Phi_Q(t) + \Phi_b(t)], \tag{74}$$

where the bath damping function is described by the slowly decaying exponential term given in Eq. (69). In the term $\Phi_Q(t)$, the contributions of the Matsubara frequencies are found to be significant even at ambient temperatures and cannot be neglected. The numerical analysis of the rate constant in the weak solvation regime suggests that at least the first five to ten Matsubara frequencies should be included in

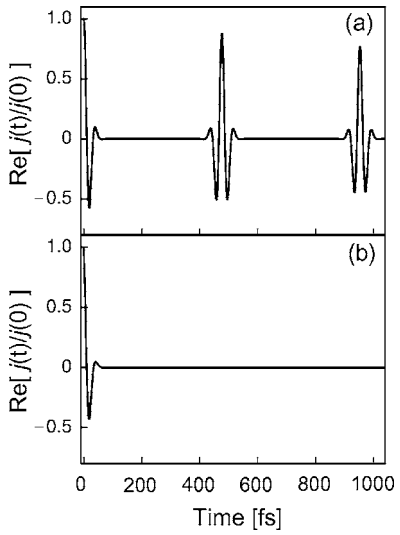

FIG. 8. Probability flux correlation function in the weak solvation regime with $\lambda_b=0.001$ kcal/mol and $\Delta_0=0$. The friction constants corresponding to the coupling between the donor-acceptor mode and the bath are (a) $\gamma=0$ and (b) $\gamma=20$ cm^{-1}. The donor-acceptor mode frequency is $\omega_0=70$ cm^{-1} and the temperature is $T=300$ K.

the calculation of $\Phi_Q(t)$ in order to achieve convergence of the numerical integration. The presence of the Matsubara frequencies prevents the analytical evaluation of the time integral of the probability flux correlation function. Thus, the rate constants presented below were obtained by numerical integration of the probability flux correlation function given in Eq. (74).

The time evolution of the normalized probability flux correlation function for $\gamma=0$ (undamped donor-acceptor mode) and $\gamma=20$ cm^{-1} is shown in Fig. 8. In contrast to the strong solvation regime, the qualitative behavior of the probability flux correlation function is significantly affected by the coupling between the donor-acceptor mode and the bath in the weak solvation regime. In the undamped case with $\gamma=0$, the probability flux correlation function exhibits slowly decaying and recurrent rapid oscillations with a recurrence period of $2\pi/\omega_0$, whereas in the damped case with $\gamma=20$ cm^{-1}, the oscillations of the probability flux correlation function are completely damped within 100 fs. This behavior is a direct manifestation of the alternative energy dissipation mechanism provided by the coupling between the donor-acceptor mode and the bath. When the donor-acceptor mode is coupled to the bath, the energy exchange between the TLS and the dissipative bath with a continuous spectrum can occur through excitation of the donor-acceptor mode. This mechanism for energy dissipation becomes predominant in the weak solvation regime and is the only channel available in the extreme case of zero bath reorganization energy $\lambda_b=0$.

The complex time dependence of the probability flux correlation function in the undamped case with $\gamma=0$ leads to anomalous oscillatory behavior of the rate constant as a function of the energy bias parameter Δ_0, as depicted in Fig. 9. The oscillations of the rate constant with a period of $\approx\hbar\omega_0$ reflect the slowly decaying recurring oscillations of the probability flux correlation function depicted in Fig. 8(a). This anomalous behavior of the rate constant in the case of $\gamma=0$ is

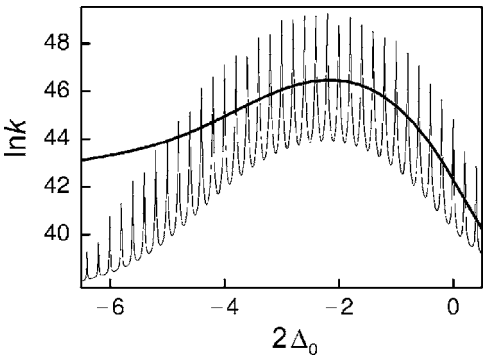

FIG. 9. Dependence of the rate constant on the energy bias $2\Delta_0$ in the weak solvation regime with $\lambda_b=0.001$ kcal/mol. The friction constants corresponding to the coupling between the donor-acceptor mode and the bath are $\gamma=0$ (oscillatory thin line) and $\gamma=20$ cm^{-1} (smooth thick line). The donor-acceptor mode frequency is $\omega_0=70$ cm^{-1} and the temperature is $T=300$ K.

a manifestation of the deficiency of the model with an undamped donor-acceptor mode in the weak solvation regime. In the case of the damped donor-acceptor mode with $\gamma=20$ cm^{-1}, however, the oscillations are completely damped, and the dependence of the rate constant on the energy bias parameter Δ_0 exhibits smooth behavior, as depicted in Fig. 9. This curve resembles a Marcus inverted parabola with clearly distinguishable inverted and normal regions. For a sufficiently damped donor-acceptor mode, the magnitude of the rate constant and the position of the maximum of the Marcus inverted parabola depend only weakly on γ in the weak solvation regime.

For lower donor-acceptor mode frequencies and higher temperatures (i.e., when $\beta\hbar\omega_0 \ll 1$), the energy exchange between the TLS and the bath is enhanced due to the population of excited states of the Q mode. In this case, the hydrogen tunneling reaction can proceed by a thermally activated process even in the weak solvation regime. The corresponding temperature dependence of the rate constant is depicted in Fig. 10.

For higher donor-acceptor mode frequencies and lower temperatures (i.e., when $\beta\hbar\omega_0 \gg 1$), the situation becomes more complicated. In this case, the donor-acceptor mode is predominantly frozen in its ground state and therefore cannot effectively participate in the energy transfer between the TLS

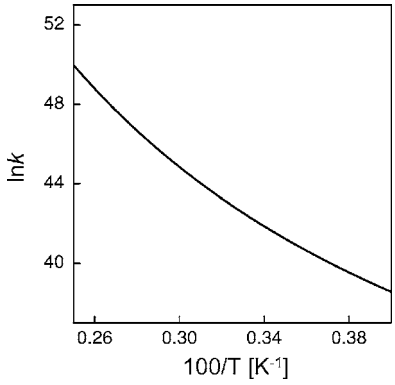

FIG. 10. Temperature dependence of the rate constant in the weak solvation regime for the case of a low donor-acceptor mode frequency $\omega_0=70$ cm^{-1}. The parameters for this model system are $\lambda_b=0.001$ kcal/mol, $\Delta_0=0$, $\gamma=20$ cm^{-1}, $\lambda_\alpha=0.43$ kcal/mol, and $\lambda_Q=0.052$ kcal/mol.

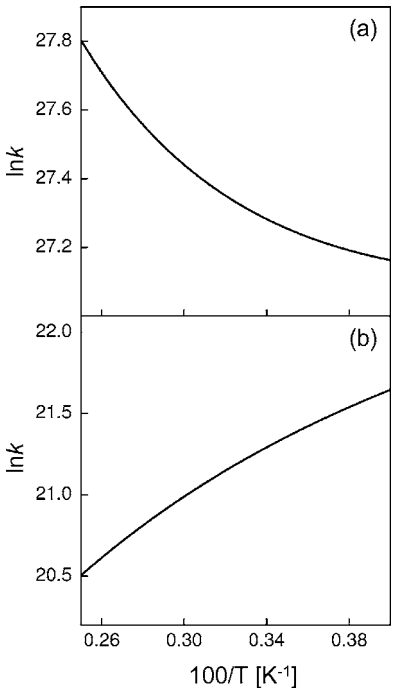

FIG. 11. Temperature dependence of the rate constant in the weak solvation regime for the case of a high donor-acceptor mode frequency $\omega_0 = 400\ \mathrm{cm}^{-1}$. The parameters that are the same for both model systems are $\lambda_b = 0.001$ kcal/mol, $\Delta_0 = 0$, and $\gamma = 20\ \mathrm{cm}^{-1}$. The other parameters are (a) $\alpha = 35\ \text{Å}^{-1}$, $\Delta Q = 0.29$ Å, $M = 20$ amu, $\lambda_\alpha = 2.95$ kcal/mol, and $\lambda_Q = 0.34$ kcal/mol and (b) $\alpha = 15\ \text{Å}^{-1}$, $\Delta Q = 0.57$ Å, $M = 40$ amu, $\lambda_\alpha = 0.27$ kcal/mol, and $\lambda_Q = 2.71$ kcal/mol.

and the bath even in the presence of coupling to the bath (i.e., when $\gamma \neq 0$). Thus, the temperature dependence of the rate constant becomes very complex and is determined by an interplay among the donor-acceptor mode frequency ω_0, the coupling between the donor-acceptor mode and the bath (quantified by the friction constant γ), the energy bias parameter Δ_0, and the relative magnitudes of λ_α and λ_Q. For example, certain combinations of these parameters may lead to an inverse temperature dependence of the rate constant. This type of complex temperature dependence of the rate is typical for low-temperature quantum tunneling processes and has been discussed previously.[28,51,52]

The complex temperature dependence of the rate constant for the extended spin-boson model is illustrated in Fig. 11. The results are shown for two combinations of the parameters λ_α and λ_Q for a model system with zero energy bias parameter $\Delta_0 = 0$ and $\gamma = 20\ \mathrm{cm}^{-1}$. When $\lambda_\alpha > \lambda_Q$, the rate increases with temperature, and the system exhibits the qualitative features of a thermally activated process. When $\lambda_\alpha < \lambda_Q$, the inverse linear temperature dependence is observed.

An estimate of how small the bath reorganization energy must be in order for the damping of the donor-acceptor mode to become important can be obtained from Eq. (67), which defines the strong and weak solvation regimes. The damping of the donor-acceptor mode is important for the convergence of the time integral probability flux correlation function in the weak solvation regime ($\Lambda \ll 1$). For a bath cut-off frequency of $\tilde{\Omega}_c = 100\ \mathrm{cm}^{-1}$ at room temperature, $\lambda_b = 0.07$ kcal/mol when $\Lambda = 1$. As shown above, we observed oscillations of the probability flux correlation function with a bath reorganization energy of $\lambda_b = 0.001$ kcal/mol in the absence of damping. Thus, we estimate that the damping of the donor-acceptor mode is important to facilitate convergence of the time integral of the probability flux correlation function when $\lambda_b < 0.01$ kcal/mol. This estimate is consistent with the previous estimate of 0.05 kcal/mol for the solvent reorganization energy sufficient to ensure convergence of a similar integral for vibrationally nonadiabatic hydrogen transfer reactions.[19,26] Anomalous temperature dependence of the rate constant was also observed in previous studies.[19,26,52] In the present paper, however, the anomalous temperature dependence is a manifestation of the qualitatively different dominant energy dissipation mechanism through excitation of the donor-acceptor mode in the weak solvation regime.

The general formulation presented here is not directly applicable to systems in which the bath reorganization energy becomes identically zero (i.e., when $\lambda_b = 0$). In the case of Ohmic dissipation, the bath damping factor $\exp[\Phi_b(t)]$ given by Eq. (69) is necessary to ensure convergence of the time integral of the probability flux correlation function. In the absence of this factor (i.e., when $\lambda_b = 0$), the probability flux correlation function reaches a constant nonzero value, namely, the square of the thermally averaged nonadiabatic coupling, at infinite time. The thermally averaged nonadiabatic coupling, which is expressed in Eq. (34), vanishes due to the infrared divergence for Ohmic spectral density if $\lambda_b \neq 0$. When $\lambda_b = 0$, however, this quantity is finite and nonzero, and its square must be subtracted from the probability flux correlation function to ensure convergence of the time integral. As a result, the perturbation theory for the total Hamiltonian must be reformulated. In particular, the unperturbed Hamiltonian should be redefined, and the dynamics of the system will contain both coherent and incoherent counterparts.[53–55] The detailed analysis of this case is beyond the scope of the present paper and will be a subject of future work.

IV. CONCLUSIONS

In this paper, we derived a nonadiabatic rate expression for hydrogen tunneling processes in the condensed phase. Our derivation is based on first-order perturbation theory for a model system described by a modified spin-boson Hamiltonian with a tunneling matrix element exponentially dependent on the hydrogen donor-acceptor distance. In this model, the TLS representing the localized reactant and product hydrogen vibrational states is linearly coupled to the donor-acceptor vibrational mode and the harmonic bath. The Hamiltonian also includes bilinear coupling between the donor-acceptor mode and the bath oscillators. This coupling provides an additional channel for energy exchange between the TLS and the bath through the donor-acceptor mode. In the weak solvation regime corresponding to small bath reorganization energies, this alternative channel facilitates convergence of the time integral of the probability flux correlation function.

We calculated the rate constant by numerical integration of the probability flux correlation function for a series of model systems with varying physical properties. For all model systems, the rate constant increases as the frequency of the donor-acceptor mode decreases because the lower frequency vibrations enable more effective sampling of the smaller donor-acceptor distances, which are associated with larger nonadiabatic couplings. In most regimes, the rate constant depends only weakly on γ, which characterizes the coupling between the donor-acceptor mode and the bath. The dependence of the rate constant on the other parameters varies for the different regimes.

In the strong solvation regime, the dominant energy exchange channel is directly between the TLS and the bath. In the high-temperature limit for the bath, the hydrogen tunneling reaction is a thermally activated process characterized by an increase in the rate constant with temperature. The dependence of the rate constant on the energy bias parameter Δ_0 resembles a slightly asymmetric Marcus inverted parabola. The coupling between the donor-acceptor mode and the bath increases the effective reorganization energy and shifts the maximum of this inverted parabola toward more negative values of Δ_0. As a result, the rate constant can either decrease monotonically with the friction constant γ or exhibit a maximum as a function of γ, depending on the value of the energy bias parameter. In either case, the dependence of the rate constant on γ is weak.

In the weak solvation regime, the channel for energy exchange between the TLS and the bath through the donor-acceptor mode becomes more important due to the small bath reorganization energy. In this case, complex temperature dependence of the rate constant can be observed. Model systems with a low-frequency donor-acceptor mode and nonzero coupling between the donor-acceptor mode and the bath (i.e., $\gamma \neq 0$) exhibit the typical temperature dependence of the rate constant for a thermally activated process, where the rate constant increases with temperature. For these systems, the energy exchange between the TLS and the bath occurs predominantly through excitation of the donor-acceptor mode. This mechanism is less effective for a high-frequency donor-acceptor mode that remains mainly in the ground state. As a consequence of the quantum character of the high-frequency donor-acceptor mode, an inverse temperature dependence of the rate constant can be observed for model systems with certain combinations of parameters in the weak solvation regime.

This study provides insight into the underlying physical principles of hydrogen tunneling processes in solution and proteins. The theoretical formulation is applicable to a wide range of chemical and biological processes, including neutral hydrogen transfer reactions with small solvent reorganization energies. These types of calculations assist in the interpretation of unusually high deuterium kinetic isotope effects and complex temperature dependence of the rates and kinetic isotope effects.

ACKNOWLEDGMENTS

This work was supported by NSF Grant No. CHE-05-01260 and NIH Grant No. GM56207. One of the authors (Y.O.) is grateful for the support by the Japanese Society for the Promotion of Science Postdoctoral Fellowships for Research Abroad.

APPENDIX A: DERIVATION OF COUNTERTERM

In this appendix, we discuss the origin of the counterterm $\Delta U(Q)$ added to the spin-boson Hamiltonian in Eq. (6). The total potential energy in the Hamiltonian given in Eq. (6) is given by

$$U_\sigma(Q,\{q_j\}) = -\Delta_0\sigma_z + \frac{1}{2}M\omega_0^2\left(Q + \frac{f\sigma_z}{M\omega_0^2}\right)^2 + \sum_{j=1}^{N}\frac{1}{2}m_j\omega_j^2\left(q_j + \frac{f_j\sigma_z}{m_j\omega_j^2}\right)^2 + \sum_{j=1}^{N} C_j\left(Q + \frac{f\sigma_z}{M\omega_0^2}\right)\left(q_j + \frac{f_j\sigma_z}{m_j\omega_j^2}\right) + \Delta U(Q). \tag{A1}$$

Comparison of Eq. (A1) to Eq. (4) reveals that these potential energies are identical except for the counterterm if the following relations hold:

$$E_R(\bar{Q}_R,\{\bar{q}_R^{(j)}\}) = -\Delta_0, \quad E_P(\bar{Q}_P,\{\bar{q}_P^{(j)}\}) = \Delta_0,$$

$$\bar{Q}_R = -\frac{f}{M\omega_0^2}, \quad \bar{Q}_P = \frac{f}{M\omega_0^2}, \tag{A2}$$

$$\bar{q}_R^{(j)} = -\frac{f_j}{m_j\omega_j^2}, \quad \bar{q}_P^{(j)} = \frac{f_j}{m_j\omega_j^2}.$$

The counterterm $\Delta U(Q)$ has been included in Eq. (A1) to compensate for the renormalization of the Q-mode frequency arising from the addition of the Q-mode-bath interaction term, which is the fourth term in Eq. (A1).

In the absence of the counterterm, the potential energy surface can be expressed as

$$\begin{aligned} U_\sigma(Q,\{q_j\}) &= -\Delta_0\sigma_z + \frac{1}{2}M\omega_0^2(Q-\bar{Q}_\sigma)^2 + \sum_{j=1}^{N}\frac{1}{2}m_j\omega_j^2(q_j-\bar{q}_\sigma^{(j)})^2 + \sum_{j=1}^{N} C_j(Q-\bar{Q}_\sigma)(q_j-\bar{q}_\sigma^{(j)}) \\ &= -\Delta_0\sigma_z + \frac{1}{2}M\omega_0^2(Q-\bar{Q}_\sigma)^2 + \sum_{j=1}^{N}\frac{1}{2}m_j\omega_j^2\left[q_j-\bar{q}_\sigma^{(j)} + \frac{C_j}{m_j\omega_j^2}(Q-\bar{Q}_\sigma)\right]^2 - \sum_{j=1}^{N}\frac{C_j^2}{2m_j\omega_j^2}(Q-\bar{Q}_\sigma)^2, \end{aligned} \tag{A3}$$

where the displacements of the environmental oscillators are expressed as $\bar{Q}_\sigma$ and $\bar{q}_\sigma^{(j)}$ for the Q and bath oscillators using

Eqs. (A2). For a given Q, the minimum of the surface $U_\sigma(Q,\{q_j\})$ is located at $\tilde{q}_\sigma^{(j)}=\bar{q}_\sigma^{(j)}-C_j/m_j\omega_j^2(Q-\bar{Q}_\sigma)$ for all j. The path along $\tilde{q}_\sigma^{(j)}$ gives the effective potential energy surface with respect to the coordinate Q as

$$U_\sigma(Q,\{\tilde{q}_\sigma^{(j)}\}) \equiv U_\sigma^{\mathrm{eff}}(Q) = \frac{1}{2}M\omega_0^2(Q-\bar{Q}_\sigma)^2 - \sum_{j=1}^{N}\frac{C_j^2}{2m_j\omega_j^2}(Q-\bar{Q}_\sigma)^2. \tag{A4}$$

The second term in the above equation leads to a renormalization of the squared frequency ω_0^2 according to

$$\tilde{\omega}^2 = \omega_0^2 - \sum_{j=1}^{N}\frac{C_j^2}{Mm_j\omega_j^2}. \tag{A5}$$

The renormalization term can be larger than ω_0^2, and the resulting frequency $\tilde{\omega}$ can become imaginary. To compensate for this renormalization effect in the total Hamiltonian, we add the counterterm

$$\Delta U(Q) = \sum_{j=1}^{N}\frac{C_j^2}{2m_j\omega_j^2}(Q-\bar{Q}_\sigma)^2 = \sum_{j=1}^{N}\frac{C_j^2}{2m_j\omega_j^2}\left(Q+\frac{f\sigma_z}{M\omega_0^2}\right)^2. \tag{A6}$$

APPENDIX B: CONTOUR INTEGRATION

In this appendix, we use the contour integration approach to evaluate the integral

$$I(t) = \frac{\lambda_\alpha}{\hbar\omega_0}\int_0^\infty d\omega\xi(\omega)\cos\,\omega tL(\omega), \tag{B1}$$

which is in Eq. (47). The other integrals in Eq. (47) can be evaluated by a similar approach. Note that the integral in Eq. (B1) represents the symmetrized position autocorrelation function for a damped harmonic oscillator coupled to a dissipative bath.

The function $L(\omega)$ for the Ohmic spectral density with the Drude-type cutoff has the following form:

$$L(\omega) = \frac{2\omega_0}{\pi}\frac{\gamma\omega D(\omega)}{(\gamma\omega D(\omega))^2+(\omega^2-\omega_0^2)^2}, \tag{B2}$$

where

$$D(\omega) = \frac{\Omega_c^2}{\Omega_c^2+\omega^2}. \tag{B3}$$

For a large cut-off frequency $\Omega_c \gg \omega_0$, $L(\omega)$ can be approximated as

$$L(\omega) \approx \frac{2\omega_0}{\pi}\frac{\gamma\omega D(\omega)}{\gamma^2\omega^2+(\omega^2-\omega_0^2)^2}. \tag{B4}$$

Consider the following integral over the closed contour C in the complex plane:

$$I_C(t) = \int_C dz\xi(z)e^{izt}f(z) \quad (t>0), \tag{B5}$$

where

$$f(z) = \frac{\gamma z D(z)}{(\gamma z)^2+(z^2-\omega_0^2)^2} \tag{B6}$$

is an analytic continuation of the function in Eq. (B4) in the upper complex plane. The integration contour C is a closed semicircle with radius R in the upper half of the complex plane. The path along the real axis avoids the origin by forming an infinitesimal semicircle with radius ε.

The function $f(z)$ has two simple poles in the upper half of the complex plane,

$$\omega_+ = \bar{\omega}+i\frac{\gamma}{2}, \quad \omega_- = -\bar{\omega}+i\frac{\gamma}{2}, \tag{B7}$$

where

$$\bar{\omega} = \sqrt{\omega_0^2-\frac{\gamma^2}{4}}. \tag{B8}$$

The residues associated with the poles ω_+ and ω_- are given by

$$a_+ = \lim_{z\to\omega_+}\coth\left[\frac{\beta\hbar z}{2}\right]e^{izt}f(z)(z-\omega_+) = \frac{1}{4\bar{\omega}i}e^{-(\gamma/2)t}e^{i\bar{\omega}t}\coth\left[\frac{\beta\hbar\omega_+}{2}\right], \tag{B9}$$

$$a_- = \lim_{z\to\omega_-}\coth\left[\frac{\beta\hbar z}{2}\right]e^{izt}f(z)(z-\omega_-) = -\frac{1}{4\bar{\omega}i}e^{-(\gamma/2)t}e^{i\bar{\omega}t}\coth\left[\frac{\beta\hbar\omega_-}{2}\right]. \tag{B10}$$

The residue from the pole $i\Omega_c$ originating from the Drude cut-off function $D(z)$ is

$$d_0 = \lim_{z\to i\Omega_c}\coth\left[\frac{\beta\hbar z}{2}\right]e^{izt}f(z)(z-i\Omega_c) = \frac{1}{2}\coth\left[i\frac{\beta\hbar\Omega_c}{2}\right]\frac{\gamma\Omega_c^2e^{-\Omega_c t}}{(\Omega_c^2+\omega_0^2)^2-\gamma^2\Omega_c^2}. \tag{B11}$$

The poles originating from $\xi(z)=\coth[\beta\hbar z/2]$ can be found using the series representation[56]

$$\coth z = \frac{1}{z}+2z\sum_{n=1}^{\infty}\frac{1}{\pi^2n^2+z^2}. \tag{B12}$$

These poles are located on the imaginary axis at $z_n=i\nu_n$, $n=1,2,\ldots$, where

$$\upsilon_n = \frac{2\pi n}{\beta\hbar}, \quad n=1,2,\ldots \tag{B13}$$

are the Matsubara frequencies. The corresponding residues are given by

$$b_n = \lim_{z\to i\nu_n} f(z)e^{izt}\coth\left[\frac{\beta\hbar z}{2}\right](z-i\nu_n) = \frac{2i\gamma}{\beta\hbar}\frac{D(i\nu_n)\nu_n e^{-\nu_n t}}{(\nu_n^2+\omega_0^2)^2-\gamma^2\nu_n^2}. \tag{B14}$$

According to the theorem of residues, the integral in Eq. (B5) is

$$I_C(t) = 2\pi i\left(a_+ + a_- + \sum_{n=1}^{\infty} b_n + d_0\right)$$
$$= \frac{\pi}{2\bar{\omega}} e^{i\omega_+ t}\xi(\omega_+) - \frac{\pi}{2\bar{\omega}} e^{i\omega_- t}\xi(\omega_-)$$
$$- \frac{4\pi\gamma}{\beta\hbar}\sum_{n=1}^{\infty} \frac{D(i\nu_n)\nu_n e^{-\nu_n t}}{(\nu_n^2+\omega_0^2)^2 - \gamma^2\nu_n^2}$$
$$+ \pi i\xi(i\Omega_c)\frac{\gamma\Omega_c^2 e^{-\Omega_c t}}{(\Omega_c^2+\omega_0^2)^2 - \gamma^2\Omega_c^2}. \quad \text{(B15)}$$

The integral over the contour C can be expressed as a sum of integrals over the following four paths:

$$I_C = I_{C_-} + I_{C_+} + I_{C_\varepsilon} + I_{C_R}, \quad \text{(B16)}$$

where I_{C_R} and I_{C_ε} are the integrals along the semicircles of radius R and infinitesimal radius ε, respectively, and $I_{C_-} + I_{C_+}$ is the sum of the integrals along the negative and positive parts of the real axis (i.e., the principal value integral). In the limits of $R\to\infty$ and $\varepsilon\to 0$, the integrals along the semicircles vanish and

$$I_C(t) = \int_{-\infty}^{\infty} f(z)\xi(z)\cos ztdz. \quad \text{(B17)}$$

Thus,

$$I(t) = \frac{\lambda_\alpha}{\pi\hbar} I_C(t)$$
$$= \frac{\lambda_\alpha}{2\hbar\bar{\omega}} e^{-(\gamma/2)t}[e^{i\bar{\omega}t}\xi(\omega_+) - e^{-i\bar{\omega}t}\xi(\omega_-)]$$
$$- \frac{4\lambda_\alpha\gamma}{\beta\hbar^2}\sum_{n=1}^{\infty} \frac{D(i\nu_n)\nu_n e^{-\nu_n t}}{(\nu_n^2+\omega_0^2)^2 - \gamma^2\nu_n^2}$$
$$+ \frac{\lambda_\alpha}{\hbar}\xi(i\Omega_c)\frac{i\gamma\Omega_c^2 e^{-\Omega_c t}}{(\Omega_c^2+\omega_0^2)^2 - \gamma^2\Omega_c^2}. \quad \text{(B18)}$$

[1] K. M. Doll, B. R. Bender, and R. G. Finke, J. Am. Chem. Soc. **125**, 10877 (2003).
[2] K. M. Doll and R. G. Finke, Biochemistry **40**, 8653 (2001).
[3] K. M. Doll and R. G. Finke, Inorg. Chem. **42**, 4849 (2003).
[4] M. J. Knapp and J. P. Klinman, Eur. J. Biochem. **269**, 3113 (2002).
[5] M. J. Knapp, K. Rickert, and J. P. Klinman, J. Am. Chem. Soc. **124**, 3865 (2002).
[6] K. Rickert and J. P. Klinman, FASEB J. **13**, A1529 (1999).
[7] K. W. Rickert and J. P. Klinman, Biochemistry **38**, 12218 (1999).
[8] E. Hatcher, A. V. Soudackov, and S. Hammes-Schiffer, J. Am. Chem. Soc. **126**, 5763 (2004).
[9] A. O. Caldeira and A. J. Leggett, Ann. Phys. (N.Y.) **149**, 374 (1983).
[10] A. J. Leggett, S. Chakravarty, A. T. Dorsey, M. P. A. Fisher, A. Garg, and W. Zwerger, Rev. Mod. Phys. **59**, 1 (1987).
[11] R. Kubo and Y. Toyozawa, Prog. Theor. Phys. **13**, 160 (1955).
[12] M. Bixon and J. Jortner, J. Chem. Phys. **48**, 715 (1968).
[13] R. A. Marcus, J. Chem. Phys. **24**, 966 (1956).
[14] V. G. Levich and R. R. Dogonadze, Dokl. Akad. Nauk SSSR **124**, 123 (1959).
[15] R. A. Marcus and N. Sutin, Biochim. Biophys. Acta **811**, 265 (1985).
[16] M. Bixon and J. Jortner, *Electron Transfer-From Isolated Molecules To Biomolecules* (Wiley, New York, 1999), Pt. 1, Vol. 106, p. 35.
[17] A. Warshel, *Computer Modeling of Chemical Reactions in Enzymes and Solutions* (Wiley, New York, 1991).
[18] A. M. Kuznetsov, *Charge Transfer in Physics, Chemistry and Biology: Physical Mechanisms of Elementary Processes and an Introduction to the Theory* (Gordon and Breach, Amsterdam, 1995).
[19] D. Borgis and J. T. Hynes, Chem. Phys. **170**, 315 (1993).
[20] A. Staib, D. Borgis, and J. T. Hynes, J. Chem. Phys. **102**, 2487 (1995).
[21] A. Soudackov and S. Hammes-Schiffer, J. Chem. Phys. **111**, 4672 (1999).
[22] M. V. Basilevsky and M. V. Vener, Russ. Chem. Rev. **72**, 1 (2003).
[23] B. Fain, *Theory of Rate Processes in Condensed Media* (Springer, Heidelberg, 1980).
[24] L. I. Trakhtenberg, V. L. Klochikhin, and S. Y. Pshezhetsky, Chem. Phys. **69**, 121 (1982).
[25] R. I. Cukier and M. Morillo, J. Chem. Phys. **91**, 857 (1989).
[26] D. C. Borgis, S. Y. Lee, and J. T. Hynes, Chem. Phys. Lett. **162**, 19 (1989).
[27] D. Borgis and J. T. Hynes, J. Chem. Phys. **94**, 3619 (1991).
[28] A. Suarez and R. Silbey, J. Chem. Phys. **94**, 4809 (1991).
[29] G. K. Ivanov, M. A. Kozhushner, and L. I. Trakhtenberg, J. Chem. Phys. **113**, 1992 (2000).
[30] A. M. Kuznetsov and J. Ulstrup, Can. J. Chem. **77**, 1085 (1999).
[31] P. M. Kiefer and J. T. Hynes, J. Phys. Chem. A **108**, 11793 (2004).
[32] P. M. Kiefer and J. T. Hynes, J. Phys. Chem. A **108**, 11809 (2004).
[33] E. Hatcher, A. Soudackov, and S. Hammes-Schiffer, Chem. Phys. **319**, 93 (2005).
[34] E. Hatcher, A. Soudackov, and S. Hammes-Schiffer, J. Phys. Chem. B **109**, 18565 (2005).
[35] J. S. Mincer and S. D. Schwartz, J. Chem. Phys. **120**, 7755 (2004).
[36] P. Banacky, Chem. Phys. **141**, 249 (1990).
[37] A. Soudackov, E. Hatcher, and S. Hammes-Schiffer, J. Chem. Phys. **122**, 014505 (2005).
[38] A. Messiah, *Quantum Mechanics* (North-Holland, Amsterdam/ Interscience, New York, 1961).
[39] C. Cohen-Tannoudji, J. Dupont-Roc, and G. Grynberg, *Atom-Photon Interactions: Basic Processes and Applications* (Wiley, New York, 1998).
[40] S. Mukamel, *Principles of Nonlinear Optical Spectroscopy* (Oxford University Press, New York, 1995).
[41] M. Galperin, D. Segal, and A. Nitzan, J. Chem. Phys. **111**, 1569 (1999).
[42] A. Soudackov and S. Hammes-Schiffer, J. Chem. Phys. **113**, 2385 (2000).
[43] I. G. Lang and Y. A. Firsov, Sov. Phys. JETP **16**, 1301 (1963).
[44] T. Holstein, Ann. Phys. (N.Y.) **8**, 325 (1959).
[45] R. A. Harris and R. Silbey, J. Chem. Phys. **83**, 1069 (1985).
[46] R. Mazo and M. Girardeau, *Advances in Chemical Physics* (Wiley, New York, 1973), Vol. 24.
[47] U. Fano, Phys. Rev. **124**, 1866 (1961).
[48] M. Rosenau da Costa, A. O. Caldeira, S. M. Dutra, and H. Westfahl, Jr., Phys. Rev. A **61**, 022107 (2000).
[49] U. Weiss, *Quantum Dissipative Systems*, 2nd ed. (World Scientific, Singapore, 1999).
[50] A. Garg, J. N. Onuchic, and V. Ambegaokar, J. Chem. Phys. **83**, 4491 (1985).
[51] R. Silbey and R. A. Harris, J. Phys. Chem. **93**, 7062 (1989).
[52] M. Morillo and R. I. Cukier, J. Chem. Phys. **92**, 4833 (1990).
[53] P. E. Parris and R. Silbey, J. Chem. Phys. **83**, 5619 (1985).
[54] D. Segal and A. Nitzan, Chem. Phys. **281**, 235 (2002).
[55] A. Chin and M. Turlakov, Phys. Rev. B **73**, 075311 (2006).
[56] M. Abramowitz and I. A. Stegun, *Handbook of Mathematical Functions with Formulas, Graphs, and Mathematical Tables* (Wiley, New York, 1972).